

Anisotropy of persistent photoconductivity in oxygen-deficient $\text{YBa}_2\text{Cu}_3\text{O}_x$ thin films

C. Stockinger, W. Markowitsch, and W. Lang

Institut für Materialphysik der Universität Wien and Ludwig Boltzmann Institut für Festkörperphysik, Kopernikusgasse 15, A-1060 Wien, Austria

R. Rössler, J. D. Pedarnig, and D. Bäuerle

Angewandte Physik, Johannes-Kepler-Universität Linz, A-4040 Linz, Austria

(Received 14 September 1998; revised manuscript received 2 March 1999)

$\text{YBa}_2\text{Cu}_3\text{O}_x$ ($x \approx 6.6$) thin films were deposited by pulsed-laser ablation on SrTiO_3 substrates, that were cut with a tilt angle $\alpha = 10^\circ$ with respect to the [001] direction, inducing a steplike growth of the CuO_2 layers. The films appeared semiconducting along the projection of the c axis to the film surface, but metallic in the perpendicular direction. From the anisotropic resistance, the in-plane (ρ_{ab}) and the out-of-plane (ρ_c) resistivities were calculated. Photodoping with white light was performed at various temperatures from 70–305 K. We have found strongly temperature dependent photoinduced decreases of ρ_{ab} and ρ_c . At low temperatures, the relative reduction of ρ_c was smaller than that of ρ_{ab} , whereas, near room temperature, they were nearly the same. The electrical anisotropy ρ_c/ρ_{ab} increased monotonously at 70 K, but, at higher temperatures, a fast increase was followed by a long-term decay. This unusual behavior resembles that of the in-plane Hall mobility in a previous study, suggesting that both quantities are changed by the same physical process. The results are discussed within the models previously proposed for the photodoping effect in $\text{YBa}_2\text{Cu}_3\text{O}_x$.
[S0163-1829(99)11833-2]

I. INTRODUCTION

Persistent photoconductivity (PPC), reported by Kudinov *et al.*,¹ is a well-known phenomenon in oxygen depleted $\text{YBa}_2\text{Cu}_3\text{O}_x$. It has been established that long-term excitation by visible radiation causes significant changes of the normal-state and superconducting transport properties,^{1–6} the optical spectra,⁷ and the electrical properties of grain-boundary Josephson junctions.^{8–10} Most experimental studies of this remarkable effect were performed on c -axis oriented thin films of $\text{YBa}_2\text{Cu}_3\text{O}_x$, and, hence were restricted to measurements of the in-plane properties. However, x-ray studies^{11,12} and magnetotransport experiments¹³ indicated pronounced changes of the structural and electronic anisotropy of the material. From these results, one can expect that the electrical anisotropy of the samples must also be affected by long-term light exposure. However, this is difficult to prove, since single crystals are hardly suitable for photodoping experiments due to the small optical penetration depth in $\text{YBa}_2\text{Cu}_3\text{O}_x$, which is of the order of about 100 nm.

We have shown in a previous paper¹⁴ that this difficulty can be overcome by using specially prepared YBCO thin films, deposited on “wedged” substrates. These films show a steplike growth with the crystallographic c axis slanted with respect to the surface normal.^{15–17} As a result, electrical currents flowing along the projection of the c axis to the film surface (in the following we will call this direction the “tilt direction”) have a component *parallel* to the c -axis direction. In the perpendicular direction, the current propagates along the a - b planes. From measurements of the resistance in both principal current directions, the in-plane as well as the out-of-plane resistivities, ρ_{ab} and ρ_c , can easily be calculated.

Using these films, we demonstrated in Ref. 14 that the

PPC effect indeed exists along the c -axis direction in $\text{YBa}_2\text{Cu}_3\text{O}_x$. We observed similar photoinduced conductivity enhancements in the a - b - and c -axis directions near room temperature. Here, we extend these studies in a systematic way by investigating the effect of illumination on the electrical anisotropy and on the shape of the ρ_c vs temperature characteristics at various temperatures between the superconducting transition temperature and room temperature. These experiments were stimulated by the results of our previous magnetotransport studies⁶ that indicated qualitatively different processes involved in the photodoping process at different temperatures. In these studies, however, the role of the so-called *photoassisted oxygen ordering* process^{3,4,18} could not be determined unambiguously. With the additional information about the photoinduced changes of the out-of-plane resistivity, provided by the present study, we can give a far more reliable picture of the photodoping process in $\text{YBa}_2\text{Cu}_3\text{O}_x$.

II. SAMPLE PREPARATION AND MEASUREMENT TECHNIQUES

$\text{YBa}_2\text{Cu}_3\text{O}_x$ thin films were grown by pulsed-laser deposition (KrF-excimer laser, $\lambda = 248$ nm, fluence 3.25 J cm^{-2} , pulse duration 25 ns, repetition rate 10 Hz) on “wedged” SrTiO_3 substrates.^{15–17} The term “wedged” means that the substrates were cut with a tilt angle α with respect to the [001] direction (lower panel in Fig. 1). For the present work, we used $\alpha = 10^\circ$. During the deposition, the substrates were kept at 760°C in an oxygen atmosphere of 0.2 mbar. Afterwards, the films were annealed for 100 min keeping the oxygen pressure unchanged. The films showed a superconducting transition at $T_{c0} \approx 56$ K, corresponding to an oxygen content of $x \approx 6.6$.¹⁸ The last preparation step was the fabri-

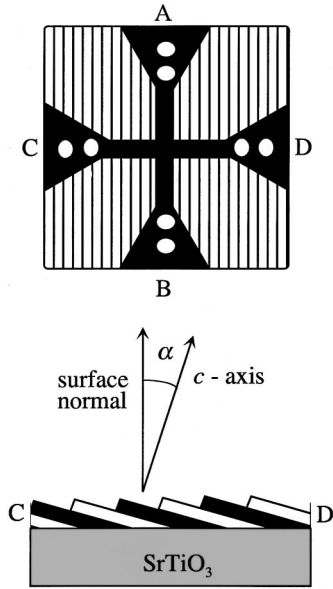


FIG. 1. Schematic illustration of the $\text{YBa}_2\text{Cu}_3\text{O}_x$ samples used in our experiments. Upper panel: Crosslike-shaped test structure. The vertical lines symbolize the intersections of the (001) planes with the surface. Lower panel: cross section of the samples showing the steplike growth of the films. α is the tilt angle and CD is the “tilt direction” of the film.

cation of a cross-shaped test structure by means of photolithography and wet chemical etching. One bridge of the cross was parallel and the other one perpendicular to the tilt direction. Four silver contact pads were evaporated on each of the bridges making the structure suitable for resistance measurements in the two principal directions of the electrical current (see Fig. 1, upper panel).

For the photodoping experiments, the samples were mounted in a temperature controlled closed-cycle refrigerator on a cold finger. A Suprasil window allowed the illumination of the sample. The electrical resistivity was measured with a standard four-point method by using a highly stable ac current source and lock-in technique. For the illumination, a 100-W quartz tungsten halogen lamp was used, providing an estimated light intensity of 1 W cm^{-2} at the sample surface. Sample heating was reduced by a water filter placed in the optical path. The setup was fully computer controlled and, during light excitation, the resistivity was monitored every 1.4 min. For temperature control, a platinum sensor was mounted in the vicinity of the sample. The initial temperature rise ($\approx 0.5 \text{ K}$) after switching on the lamp could be nullified within a few minutes by the computer control.

Using this setup, we measured the time dependences of the resistance in the two principal current directions during illumination for 25 h at 70, 100, 160, and 275 K. At first, the sample was contacted at the pads in the CD direction and the time evolution of the resistance was measured during photoexcitation at a certain temperature. After termination of the illumination, the sample was slowly cooled down from the temperature at which the photodoping was performed to 40 K to determine T_{c0} and the shape of the ρ_c vs temperature characteristics. Then, the sample was warmed up to room temperature and kept there for 24 h to allow the complete relaxation of the PPC. After that, the cycle was repeated with

the photoexcitation performed at a different temperature. During the cooldown we carefully examined that the resistance vs temperature curve was identical with the characteristics of the undoped sample to ensure that the PPC relaxation was complete. Later, the sample was contacted in the AB direction and the above described measurement cycle was repeated in this configuration.

Some additional measurements at 260, 275, and 305 K were performed using another setup. In this case, the sample was placed in a vacuum chamber, equipped with a fused silica window, on a Peltier cooler. The light intensity and illumination time were the same as in the other series of measurements, but the Peltier cooler enabled sample cooling only down to about 250 K. We carefully examined that the resistance measurements during the illumination at 275 K, taken in both experimental setups, agreed within the experimental error, thereby confirming that the results were reproducible.

III. RESULTS

A. Calculation of ρ_c and ρ_{ab} from the resistance measurements

Figure 1 (upper panel) shows the crosslike test structure of our samples schematically. One bridge is perpendicular (AB) and the other parallel (CD) to the tilt direction. We have shown in Ref. 14 that the resistance R_{AB} (subscripts denote the current direction) displays a metallic behavior, whereas R_{CD} appears to be semiconductorlike. The reason is that an electrical current flowing through the sample in the CD direction has a component parallel to the intrinsic c -axis direction of the film, as illustrated by the lower panel in Fig. 1. Although, at a tilt angle of $\alpha = 10^\circ$, the c component is smaller than the a - b component, the temperature dependence of R_{CD} is dominated by ρ_c because of the large intrinsic anisotropy of $\text{YBa}_2\text{Cu}_3\text{O}_x$ ($\rho_c/\rho_{ab} \approx 100$ at room temperature¹⁹). From the rotation of the resistivity tensor, we get

$$R_{AB} = \frac{l}{wd} \rho_{ab}, \quad (1)$$

and

$$R_{CD} = \frac{l}{wd} (\rho_{ab} \cos^2 \alpha + \rho_c \sin^2 \alpha), \quad (2)$$

where l , w , and d denote the length, width, and thickness of the bridges ($l = 2.3 \text{ mm}$, $w = 0.1 \text{ mm}$, $d \approx 200 \text{ nm}$). Thus from the measurements of R_{AB} and R_{CD} the principal components of the resistivity tensor ρ_{ab} and ρ_c can be calculated. The validity of this evaluation method is strongly supported by the excellent agreement with single-crystal data.^{14,19} A possible influence of the defect microstructure on the measured anisotropy, which was observed in fully oxygenated YBCO thin films on tilted substrates,²⁰ is obviously of negligible importance in our oxygen-deficient samples. The reason is, most likely, that the intrinsic electrical anisotropy is larger in oxygen-deficient YBCO than in optimally doped YBCO. ρ_c/ρ_{ab} varies from about 1500–100 between 100 K and room temperature in the former,¹⁹ compared to about 80–50 in the latter.²¹

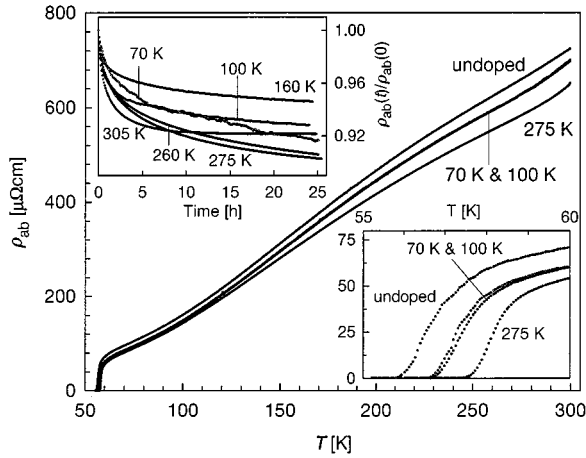


FIG. 2. ρ_{ab} vs temperature characteristics of $\text{YBa}_2\text{Cu}_3\text{O}_x$ before and immediately after white-light illumination for 25 h at the indicated temperatures. The lower inset shows the transition region on enlarged scales. Upper inset: time dependence of $\rho_{ab}(t)/\rho_{ab}(0)$ during the photodoping at the indicated temperatures.

B. The impact of photoexcitation on the anisotropic transport properties of $\text{YBa}_2\text{Cu}_3\text{O}_x$

Using Eqs. (1) and (2), we calculated the time dependences of ρ_{ab} and ρ_c as a function of the illumination time from *in situ* measurements of R_{AB} and R_{CD} at 70, 100, 160, 260, 275, and 305 K. Up to 275 K, $\rho_{ab}(t)/\rho_{ab}(0)$ showed essentially the same behavior as in conventionally grown $\text{YBa}_2\text{Cu}_3\text{O}_x$ films [compare the results in Fig. 2 (upper inset) with Ref. 6]. The ρ_{ab} reduction after 25 h of illumination was large at high temperatures (about 9–10% at 275 and 260 K) and *also* at the lowest studied temperature (about 8% at 70 K), but smaller at intermediate temperatures (about 7% at 100 K and 5% at 160 K). Only at 305 K a saturation at about 8% was observed, obviously reflecting the balance between the photodoping effect and the PPC relaxation.²² At the other studied temperatures, no real saturation of photodoping was achieved, in agreement with our previous studies.^{6,22,23} We have shown in Ref. 22 that even after 50–60 h of white-light illumination a further reduction of ρ_{ab} is observable, especially when the data are plotted on a logarithmic time scale and even if the linear plot suggests saturation. Therefore we cannot completely rule out that the dependences of the physical properties on the “photodoping temperature” (i.e., the temperature where the photodoping is carried out), which we will discuss below, are partially due to the fact that photodoping for 25 h ends up at different distances from saturation at different temperatures. However, the present as well as the previous results clearly demonstrate that the resistance drop after about 20 h of excitation becomes very slow at all temperatures so that the differences between ρ_{ab} (25 h) and the saturation value of ρ_{ab} should not vary too much from temperature to temperature.

The ρ_{ab} vs temperature characteristics, measured after the photodoping experiments and plotted in the main panel of Fig. 2, showed essentially the same behavior as in conventionally grown samples.²³ The T_{c0} enhancement was about 1 K after photodoping at 70, 100, and 160 K, but approximately two times *larger* at 275 K (see the lower inset in Fig. 2; the curve for the 160-K measurement lies between the 70

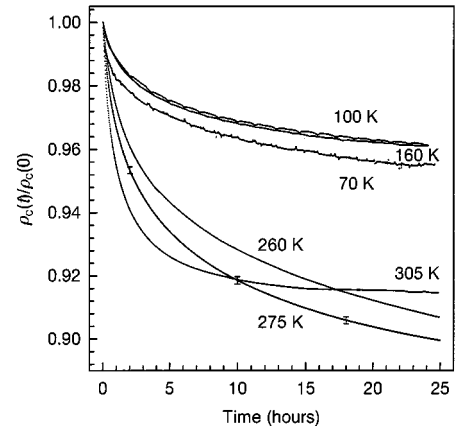


FIG. 3. Time dependence of the normalized out-of-plane resistivity $\rho_c(t)/\rho_c(0)$ of $\text{YBa}_2\text{Cu}_3\text{O}_x$ during white-light illumination at the indicated temperatures.

and 100 K curves and is therefore not displayed in the figure). We again note the excellent agreement with the previous results from conventionally grown samples.^{6,23}

The temperature dependence of $\rho_c(t)/\rho_c(0)$ showed a completely different behavior (Fig. 3). At low and intermediate temperatures (70, 100, and 160 K), the resistivity reductions were similar (about 4–5%), but *substantially larger* at the higher temperatures (260–305 K), where values of 8–10% were measured. The 305-K characteristics were obviously affected by the PPC relaxation. The results in Fig. 3 strongly suggest that, at high temperatures, an additional contribution to the photodoping effect occurs, that is of minor importance at the lower temperatures.

To assess the reliability of the results in Fig. 3 we estimated the possible errors of ρ_c due to the above two-step measurement method. We neglected possible inaccuracies of the sample geometries and the tilt angle, since we were only interested in the photoinduced *changes* of the resistivities. Error sources like noise or temperature variations during the photodoping can be estimated from the scattering of the data points in Fig. 3. More important are the possible *systematic* errors arising from the fact that the R_{AB} and the R_{CD} values were collected in two separate experimental runs. For example, slightly different temperatures in two corresponding runs could result in incorrect absolute values of the resistances. We have simulated this effect by varying the measured values of R_{AB} and R_{CD} by 5%, which we regard as an upper limit of these errors. As a result, we obtained $\rho_c(t)$ curves that were shifted parallel to the measured one. After the normalization, all these curves collapsed with the curves in Fig. 3 within the line thicknesses, indicating that the discussed type of errors is negligible, if only the normalized values are discussed. Another type of error may arise from different light intensities on the sample surface in the two runs, caused, e.g., by slightly different settings of the halogen lamp and/or different locations of the sample in the collimated light beam. This type of error essentially results in different time scales of R_{AB} and R_{CD} , and is expected to be significant especially at the higher temperatures, where the two resistances have comparable magnitudes. The reproducibility of the light intensity in our experiments was tested experimentally, using a broadband thermopile detector. The

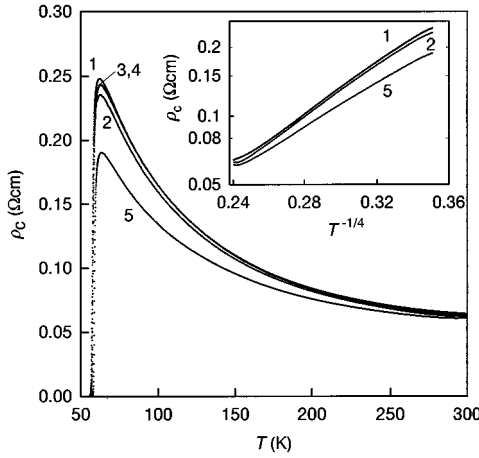


FIG. 4. ρ_c vs temperature characteristics of $\text{YBa}_2\text{Cu}_3\text{O}_x$ before and immediately after white-light illumination for 25 h (1: nonilluminated sample; 2,3,4,5: photodoped at 70, 100, 160, and 275 K, respectively). The inset shows three of the data curves plotted as $\ln \rho_c$ vs $T^{-1/4}$ between 66 and 300 K; in this plot, curves 3 and 4 collapse with curve 1.

measured values of the intensity showed deviations definitely smaller than 10%, equivalent to a maximum possible error of 20% between the two measurement runs. Hence we simulated a 20% stretching/compression of the one time scale with respect to the other. The result of the simulation is plotted as error bars to the 275 K curve in Fig. 3. Obviously, the above description of the behavior of $\rho_c(t)/\rho_c(0)$ is not questioned by the errors.

Figure 4 shows the impact of light excitation on the ρ_c vs temperature characteristics. Each curve in the figure contains two sets of measured values: the one collected during the cooldown to 40 K and the other collected during the warmup to room temperature. The absence of any thermal lag between these two branches shows that the characteristics are not influenced by the PPC relaxation. Compared to the $\rho_c(T)$ curve of the nonilluminated sample, the curves measured after the photodoping experiments at 70, 100, 160, and 275 K, appeared “compressed,” similar to the effect of high hydrostatic pressure.^{24,25} However, the inset in Fig. 4, where the curves are plotted as $\ln \rho_c$ vs $T^{-1/4}$ (the three-dimensional variable-range hopping formula), displays a remarkable difference between the effect of illumination and of pressure. As in Ref. 24, $\ln \rho_c$ in Fig. 4 (inset) is nearly linear over a wide temperature range, but, contrary to the effect of pressure, is not simply shifted parallel after photodoping. In particular, the illumination at 275 K clearly changed the slope of the curve. In the variable-range hopping picture (although its application to the out-of-plane resistivity of $\text{YBa}_2\text{Cu}_3\text{O}_x$ is somewhat problematic, as Forro *et al.*²⁴ pointed out), this implies a substantial reduction of the hopping barrier occurring mainly at high temperatures.

Of particular interest is the behavior of the electrical anisotropy of $\text{YBa}_2\text{Cu}_3\text{O}_x$ during photoexcitation. In Fig. 5, we have plotted the normalized anisotropy factor $A(t) \equiv [\rho_c(t)/\rho_c(0)]/[\rho_{ab}(t)/\rho_{ab}(0)]$ as a function of the illumination time at the studied temperatures, with error bars corresponding to the above error estimation. We observe in Fig. 5 that, at 70 K, the illumination monotonously enhanced the

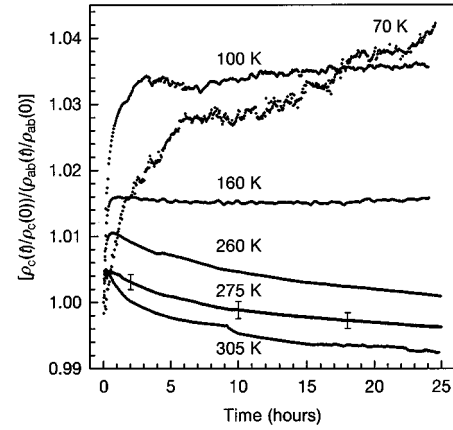


FIG. 5. Time dependence of the normalized anisotropy factor $[\rho_c(t)/\rho_c(0)]/[\rho_{ab}(t)/\rho_{ab}(0)]$ of $\text{YBa}_2\text{Cu}_3\text{O}_x$ during white-light illumination at the indicated temperatures.

anisotropy during the entire duration of the experiment. In contrast, at 100 and 160 K, $A(t)$ showed a saturation after several hours of illumination, and, at the higher temperatures, a sharp increase of $A(t)$ at the beginning of the photodoping experiment was followed by a long-term decrease. The reason for the latter is that, at high temperatures and long exposure times, $\rho_c(t)/\rho_c(0)$ decreased more rapidly than $\rho_{ab}(t)/\rho_{ab}(0)$. At both 275 and 305 K, $A(t)$ even seems to fall below 1, which implies that the prolonged photoexcitation finally resulted in a persistent *reduction* of the electrical anisotropy of the system. As an additional interesting result, different *temperature dependences* of the anisotropy, $A_\rho(T) \equiv \rho_c(T)/\rho_{ab}(T)$, were obtained after photodoping at different temperatures, with the largest differences occurring in the low-temperature range from 70–150 K (see the main panel in Fig. 6). In this range, the 70 and 100 K curves run *above*, but the 275 K curve stays *below* the “undoped” curve. This behavior of $A_\rho(T)$ is merely a consequence of the dependences of the *in-plane* (see Fig. 2) and of the *out-of-plane* (see Fig. 4) resistivity vs temperature characteristics on the photodoping temperature. The obvious conclusion is

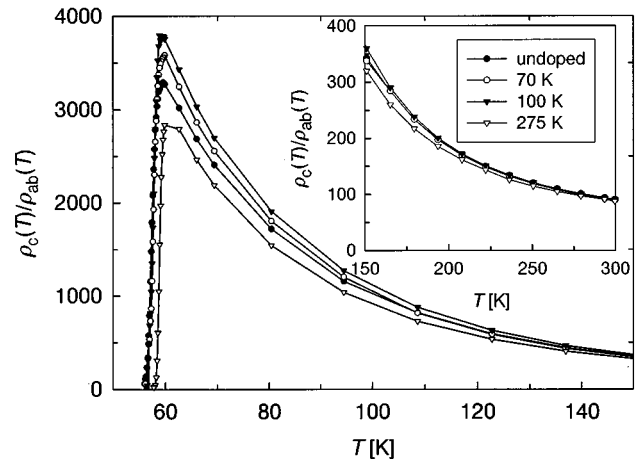


FIG. 6. Temperature dependence of the electrical anisotropy $A_\rho(T) \equiv \rho_c(T)/\rho_{ab}(T)$ of $\text{YBa}_2\text{Cu}_3\text{O}_x$ before and after white-light illumination at the indicated temperatures. Main panel: the temperature range from 50–150 K. Inset: 150–300 K.

that the nature of the photodoped state varies with the temperature at which the photoexcitation is conducted.

IV. DISCUSSION

We learn from Figs. 5 and 6 that the electrical anisotropy of $\text{YBa}_2\text{Cu}_3\text{O}_x$ is *enhanced* by prolonged photodoping at low temperatures, but is *lowered* at high temperatures. The latter effect is connected with substantial increases of the photodoping effectiveness observed in ρ_{ab} (see Fig. 2 and Ref. 6) as well as in ρ_c (see Fig. 3) and also with pronounced changes of $\rho_c(T)$ (see Fig. 4). All these findings strongly suggest that, at high temperatures, a certain photodoping process adds to others that are already working at low temperatures. Most striking is the comparison between Fig. 5 and the Hall effect data presented in Ref. 6. Obviously, the photoinduced changes of the electrical anisotropy and of the in-plane Hall mobility (μ_H) show essentially the same unusual temperature dependence. In particular, we notice the following similarities: (a) a strictly monotonous increase at low temperatures and a competition between an increasing component and a decreasing component at high temperatures is observed, (b) the positive slope at short illumination times increases with the increasing temperature, and (c) at the highest studied temperatures, both quantities fall *below* unity. Since both physical quantities are not directly connected, these results can only be understood, if the photoinduced changes of $A(t)$ and of μ_H have a common physical origin. This implies that essentially two types of mechanisms are involved in photodoping: one of them *increases* $A(t)$ and μ_H , and gives a considerable contribution at all temperatures, whereas the other one *decreases* $A(t)$ and μ_H , and shows up significantly only at high temperatures.

The decrease of $A(t)$ during photodoping at high temperatures fits well to the observed photoinduced c -axis contraction, since a reduced c -axis lattice parameter most likely implies a shorter distance between neighboring CuO_2 planes and hence a reduced energy barrier for the hopping or tunneling transport along the c -axis direction, in agreement with the curves in Figs. 4 and 5 collected at high temperatures. The c -axis contraction is consistent with *photoassisted oxygen ordering*,^{11,12} suggesting that the considered “high-temperature photodoping mechanism” can tentatively be identified with that mechanism. Another support for this assignment is provided by studies of the Hall mobility after quenching a $\text{YBa}_2\text{Cu}_3\text{O}_x$ sample from high temperatures down to room temperature, which is known to induce long-term oxygen ordering processes (“room-temperature aging”).²⁶ Nieva *et al.*⁴ observed a *decrease* of the Hall mobility during the “room-temperature aging,” which is very similar to the photoinduced decrease presented in Ref. 6. Hence, for the following discussion, we assume that the considered mechanism can be identified with *photoassisted oxygen ordering*.

In a previous paper,⁶ we have argued that only oxygen ordering can give a reasonable explanation for the observed increase of the Hall mobility at low temperatures and also during short illumination times at room temperature. This argument was based on the general consideration that an ordering process should enhance the carrier mobility. However, our new results, especially Fig. 5, suggest the modifi-

cation of this interpretation. If the oxygen ordering process was more pronounced at lower than at higher temperatures, the temperature dependence of the anisotropy should be opposite to Fig. 5. Considering the higher diffusivity of oxygen in $\text{YBa}_2\text{Cu}_3\text{O}_x$ at high temperatures,²⁷ it can be inferred from our results that the photoassisted oxygen ordering acts on the *mobile*, i.e., thermally activated oxygen across the diffusion barrier of about 1.2–1.3 eV.^{28,29} Otherwise, if the effect of photodoping carried out at, e.g., 2 eV was to activate the bounded oxygen ions, prolonged photoexcitation would finally lead to a completely disordered chain layer, which is not supported by any experimental results. On the other hand, the picture of the photoassisted oxygen ordering proposed by Osquiguil *et al.*¹⁸ may be consistent with our interpretation. They proposed that photoexcited electrons are trapped at the end of chain segments and, through local potential distortions, favor the growth of the chain segments. It seems conceivable that a thermally enhanced oxygen diffusion will facilitate this process.

In Ref. 6, we considered an “oxygen disordering” process to be responsible for the observed mobility decrease near room temperature. Within the present interpretation, however, this hypothetical process is no longer needed. Also, this picture is not in conflict with the results presented by Guimpel *et al.*,³⁰ who have shown that photodoping does not compensate for the effects of quenching-induced oxygen disorder. In their experiments, photodoping was carried out at 150 K, at which temperature, according to our interpretation, photoassisted oxygen ordering is of minor importance.

The above discussion does not include the other process, which must be mainly responsible for the photodoping at low temperatures. In the following, we examine the possibility to identify this process with one of the alternatively proposed photodoping mechanisms. The *charge-transfer models* of the PPC in $\text{YBa}_2\text{Cu}_3\text{O}_x$ assume that photoexcited electrons are transferred from the CuO_2 -plane layers to the CuO_x (chain) layers and are trapped there either in unoccupied oxygen levels² or in oxygen vacancies,^{31,32} while the mobile holes remain within the CuO_2 layers. The electron capturing is a *random* process and hence must introduce a certain amount of disorder within the chain layers. It seems quite conceivable that a disordered CuO_x layer weakens the overlap of the wave functions between neighboring CuO_2 planes and, thereby, reduces the hopping rate in the c -axis direction. As a consequence, the photoinduced reduction of ρ_c , driven by the enhancement of carrier density in the CuO_2 planes, would be delayed relatively to that of ρ_{ab} , in agreement with Fig. 5. On the other hand, the photoinduced *enhancement* of the carrier mobility can hardly be explained by a charge transfer model, so that the assignment of the process under consideration to the models proposed in Refs. 2, 31, and 32 remains questionable.

The above picture of the PPC effect seems to be contradicted by the c -axis shrinking also observed during photodoping at low temperatures.^{11,12} However, the measured relative decrease of the c -axis lattice parameter was $\approx 0.5 \times 10^{-4}$ (Refs. 11 and 12), which is three orders of magnitude smaller than the decrease of ρ_c (Fig. 3), and its impact on the electrical anisotropy may be overcompensated by the above discussed disordering of the CuO_x layers. Furthermore, in Refs. 11 and 12, insulating samples were used, in

contrast to the present studies. However, according to Fig. 3, the c -axis contraction in metallic samples should be larger after photodoping slightly below room temperature than at lower temperatures. We strongly recommend x-ray studies of the c -axis contraction as function of the photodoping temperature to prove this prediction.

ACKNOWLEDGMENT

We thank G. Heine for valuable discussions. This work was supported by the Fonds zur Förderung der wissenschaftlichen Forschung, Austria.

- ¹V. I. Kudinov, A. I. Kirilyuk, N. M. Kreines, R. Laiho, and E. Lähderanta, *Phys. Lett. A* **151**, 358 (1990).
- ²V. I. Kudinov, I. L. Chaplygin, A. I. Kirilyuk, N. M. Kreines, R. Laiho, E. Lähderanta, and C. Ayache, *Phys. Rev. B* **47**, 9017 (1993).
- ³G. Nieva, E. Osquiguil, J. Guimpel, M. Maenhoudt, B. Wuyts, Y. Bruynseraede, M. B. Maple, and I. K. Schuller, *Appl. Phys. Lett.* **60**, 2159 (1992).
- ⁴G. Nieva, E. Osquiguil, J. Guimpel, M. Maenhoudt, B. Wuyts, Y. Bruynseraede, M. B. Maple, and I. K. Schuller, *Phys. Rev. B* **46**, 14 249 (1992).
- ⁵K. Tanabe, S. Kubo, F. Hosseini Teherani, H. Asano, and M. Suzuki, *Phys. Rev. Lett.* **72**, 1537 (1994).
- ⁶C. Stockinger, W. Markowitsch, W. Lang, W. Kula, and R. Sobolewski, *Phys. Rev. B* **57**, 8702 (1998).
- ⁷K. Widder, J. Münzel, M. Göppert, D. Lürßen, R. Becker, A. Dinger, H. P. Gesserich, C. Klingshirn, M. Kläser, G. Müller-Vogt, J. Geerk, and V. M. Burlakov, *Physica C* **300**, 115 (1998).
- ⁸K. Tanabe, F. Hosseini Teherani, S. Kubo, H. Asano, and M. Suzuki, *J. Appl. Phys.* **76**, 3679 (1994).
- ⁹A. Hoffmann, I. K. Schuller, A. Gilabert, M. G. Medici, F. Schmidl, and P. Seidel, *Appl. Phys. Lett.* **70**, 2461 (1997).
- ¹⁰R. Sobolewski, R. Adam, W. Kula, W. Markowitsch, C. Stockinger, W. Göb, and W. Lang, *IEEE Trans. Appl. Supercond.* **7**, 1632 (1997).
- ¹¹K. Kawamoto and I. Hirabayashi, *Phys. Rev. B* **49**, 3655 (1994).
- ¹²D. Lederman, J. Hasen, I. K. Schuller, E. Osquiguil, and Y. Bruynseraede, *Appl. Phys. Lett.* **64**, 652 (1994).
- ¹³W. Göb, W. Lang, W. Markowitsch, V. Schlosser, W. Kula, and R. Sobolewski, *Solid State Commun.* **96**, 431 (1995).
- ¹⁴W. Markowitsch, C. Stockinger, W. Lang, K. Bierleutgeb, J. D. Pedarnig, and D. Bäuerle, *Appl. Phys. Lett.* **71**, 1246 (1997).
- ¹⁵H. Lengfellner, S. Zeuner, W. Prettel, and K. F. Renk, *Europhys. Lett.* **25**, 375 (1994).
- ¹⁶S. T. Li, A. Ritzer, E. Arenholz, D. Bäuerle, W. M. Huber, H. Lengfellner, and W. Prettl, *Appl. Phys. A: Mater. Sci. Process.* **63**, 427 (1996).
- ¹⁷D. Bäuerle, *Laser Processing and Chemistry* (Springer, Berlin, 1996).
- ¹⁸E. Osquiguil, M. Maenhoudt, B. Wuyts, Y. Bruynseraede, D. Lederman, and I. K. Schuller, *Phys. Rev. B* **49**, 3675 (1994).
- ¹⁹D. A. Brawner, Z. Z. Wang, and N. P. Ong, *Phys. Rev. B* **40**, 9329 (1989).
- ²⁰T. Haage, J. Zegenhagen, J. Q. Li, H.-U. Habermeier, M. Cardona, Ch. Jooss, R. Warthmann, A. Forkl, and H. Kronmüller, *Phys. Rev. B* **56**, 8404 (1997).
- ²¹T. A. Friedmann, M. W. Rabin, J. Giapintzakis, J. P. Rice, and D. M. Ginsberg, *Phys. Rev. B* **42**, 6217 (1990).
- ²²W. Markowitsch, C. Stockinger, W. Göb, W. Lang, W. Kula, and R. Sobolewski, *Physica C* **265**, 187 (1996).
- ²³C. Stockinger, W. Markowitsch, W. Lang, W. Kula, and R. Sobolewski, *Eur. Phys. J. B* **2**, 301 (1998).
- ²⁴L. Forro, V. Ilakovac, J. R. Cooper, C. Ayache, and J.-Y. Henry, *Phys. Rev. B* **46**, 6626 (1992).
- ²⁵M. F. Crommie, Amy Y. Liu, A. Zettl, Marvin L. Cohen, P. Parilla, M. F. Hundley, W. N. Creager, S. Hoen, and M. S. Sherwin, *Phys. Rev. B* **39**, 4231 (1989).
- ²⁶B. W. Veal, A. P. Paulikas, H. You, H. Shi, Y. Fang, and J. W. Downey, *Phys. Rev. B* **42**, 6305 (1990).
- ²⁷S. J. Rothman, J. L. Routbort, and J. E. Bakar, *Phys. Rev. B* **40**, 8852 (1989).
- ²⁸J.-P. Locquet, J. Vanacken, B. Wuyts, Y. Bruynseraede, K. Zhang, and I. K. Schuller, *Europhys. Lett.* **7**, 469 (1988).
- ²⁹S. K. Tolpygo, J.-Y. Lin, M. Gurvitch, S. Y. Hou, and J. M. Phillips, *Phys. Rev. B* **53**, 12 462 (1996).
- ³⁰J. Guimpel, B. Maiorov, E. Osquiguil, G. Nieva, and F. Pardo, *Phys. Rev. B* **56**, 3552 (1997).
- ³¹N. M. Kreines and V. I. Kudinov, *Mod. Phys. Lett. B* **6**, 289 (1992).
- ³²J. Hasen, D. Lederman, I. K. Schuller, V. I. Kudinov, M. Maenhoudt, and Y. Bruynseraede, *Phys. Rev. B* **51**, 1342 (1995).